

Electronic structure of ErSi₂ and YSi₂

L. Magaud, J. Y. Veullen, D. Lollman, and T. A. Nguyen Tan

*Laboratoire d'Etudes des Propriétés Electroniques des Solides, Centre National de la Recherche Scientifique,
25 avenue des Martyrs, Boîte Postale 166, 38042 Grenoble CEDEX 09, France*

D. A. Papaconstantopoulos and M. J. Mehl

Naval Research Laboratory, Washington, D.C. 20375-5000

(Received 25 October 1991)

We present a theoretical and experimental study of erbium and yttrium disilicides. These materials are representative of the trivalent heavy-rare-earth disilicides that can be epitaxially grown on Si(111). The densities of states are obtained using the augmented-plane-wave method. They are used to calculate the Auger Si *L*VV spectra. For the measurements, we used x-ray photoemission and Auger electron spectroscopy on monocrystalline ErSi_{1.7}. Theoretical and experimental results are compared and show structures due to Er-Si hybridization. Although the valence-band results are in qualitative agreement, we find significant differences that could be related to effects due to silicon vacancies.

I. INTRODUCTION

Heavy-rare-earth disilicides RSi_2 ($R = \text{Gd-Lu}$) and YSi_2 are very special members of the silicide family. Like CoSi_2 and NiSi_2 , they have a small lattice mismatch with Si(111) and can be epitaxially grown on it.¹ The resulting interface has a high-crystalline quality. They exhibit exceptionally low Schottky barriers on *n*-doped silicon ($\Phi_n = 0.35$ eV).² This property is very important for technological applications, especially in optics where these materials could be used in infrared detectors. It is also interesting from a fundamental point of view to understand such a low Schottky barrier. Despite these promising properties, only a few studies³⁻⁹ of their electronic structure have been performed.

The heavy-rare-earth disilicides, which can be epitaxially grown on Si(111), as well as YSi_2 , have a hexagonal structure of the $A1B_2$ type.¹ Except for Yb, these rare earths are trivalent and so their silicides have the same electronic configuration. One can therefore expect these materials to have very similar properties. Yttrium has no *f* electrons but it is generally associated with the rare earths due to its similar physical and chemical properties. Thus, YSi_2 and ErSi_2 are representative of the whole trivalent heavy-rare-earth disilicides family and their study will provide information valid for all of them.

The $A1B_2$ structure is formed by alternate planes of rare earth and silicon atoms. It gives a layered character to these materials peculiar to rare-earth disilicides. Furthermore, they are not stoichiometric but contain up to 20% of silicon vacancies.^{1,10}

In this paper, we present a theoretical study of the electronic structure of ErSi_2 together with one for YSi_2 using the self-consistent augmented-plane-wave (APW)¹¹ band calculations. X-ray photoemission (XPS) and Auger electron spectra (AES) of ErSi_2 are also presented. Then the experimental results (XPS) are compared to the theoretical density of states (DOS) and the Auger spectra to a calculated one.

II. THEORY

We shall first present the calculation procedure and then the APW results.

A. APW calculation

We have performed a self-consistent, scalar-relativistic APW calculation in the muffin-tin approximation for ErSi_2 and YSi_2 in the hexagonal $A1B_2$ structure with no silicon vacancy. The lattice constants used were $a = 3.78$ Å and $c = 4.09$ Å for ErSi_2 and $a = 3.84$ Å and $c = 4.14$ Å for YSi_2 . The calculation uses the muffin-tin approximation with touching spheres. The muffin-tin radii are $R_Y = 1.921$ Å and $R_{Si} = 1.109$ Å for YSi_2 and $R_{Er} = 1.899$ Å and $R_{Si} = 1.096$ Å for ErSi_2 .

The scalar-relativistic APW calculation includes the mass velocity and Darwin terms in the Hamiltonian but neglects the spin-orbit coupling. The $\text{Er}(6s, 6p, 5d)/\text{Y}(5s, 5p, 4d)$ and $\text{Si}(3s, 3p)$ levels are treated as valence states. Y has no *f* electrons. We forced the Er 4*f* states in the core because they have been experimentally shown to be corelike. The core levels were not frozen but they were recalculated using a fully relativistic atomic code at each iteration. The exchange and correlation potential was treated within the local-density approximation using the Hedin-Lundqvist formula.¹²

Self-consistency was reached on a mesh of 15 *k* points in the reduced Brillouin zone (RBZ)—60 *k* points in the whole zone after 20 iterations when the Fermi level converged within 1 mRy. The self-consistent potential was then used to perform the last iteration with 45 *k* points in the RBZ—384 in the whole zone. The eigenvalues were used to calculate the DOS with the tetrahedron method.¹³

B. Auger spectrum calculation

At first approximation, the Auger Si *L*VV intensity is given by the self-convolution of the silicon DOS built on

Si *s* [$N(E)_{\text{Si } s}$] and Si *p* [$N(E)_{\text{Si } p}$] partial DOS according to

$$N(E)_{\text{Si}} = N(E)_{\text{Si } p} + 0.3N(E)_{\text{Si } s} . \quad (1)$$

The 0.3 factor gives a measure of the *s*-electron participation in the transition.¹⁴

The Auger spectrum is then given by

$$\int_{\epsilon_F}^{\epsilon_b} N_{\text{Si}}(\epsilon)N_{\text{Si}}(E-\epsilon)d\epsilon . \quad (2)$$

ϵ_F is the Fermi level and ϵ_b the bottom of the band.

C. APW results

The total and partial APW densities of states of ErSi₂ inside the muffin-tin spheres are presented in Fig. 1. The reader examining this figure should first note the variable scale used for the various components of the DOS. The Si partial DOS are given for one silicon atom. As one can see from the partial DOS, the total DOS is divided into three energy regions. The first one extends from -2 to 4.5 eV and has a strong Si *s* character. The second one, from 4.5 to 6.5 eV, is mainly of Si *p* character. The third region, up to the Fermi level ($E_F=11.71$ eV), is composed of strongly hybridized Si *p* and Er *d* states. The Er *d* character increases near the Fermi level, con-

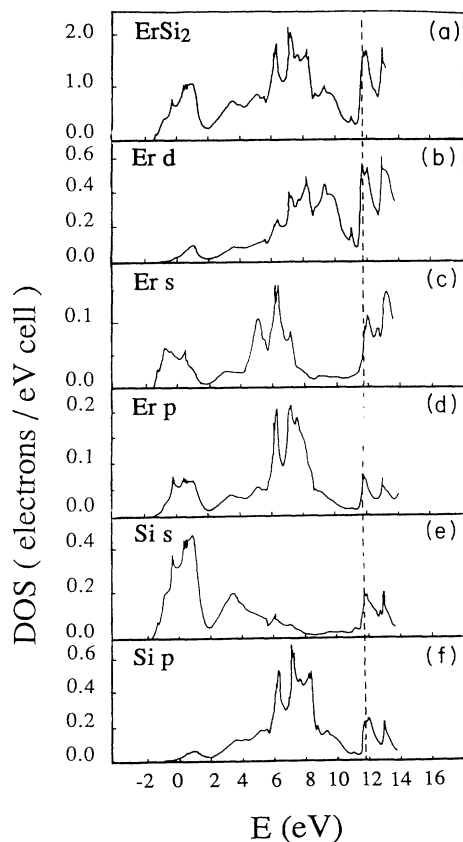


FIG. 1. APW densities of states for ErSi₂. Note the variable scale for the different angular momentum components. The Si partial DOS are given for one silicon atom.

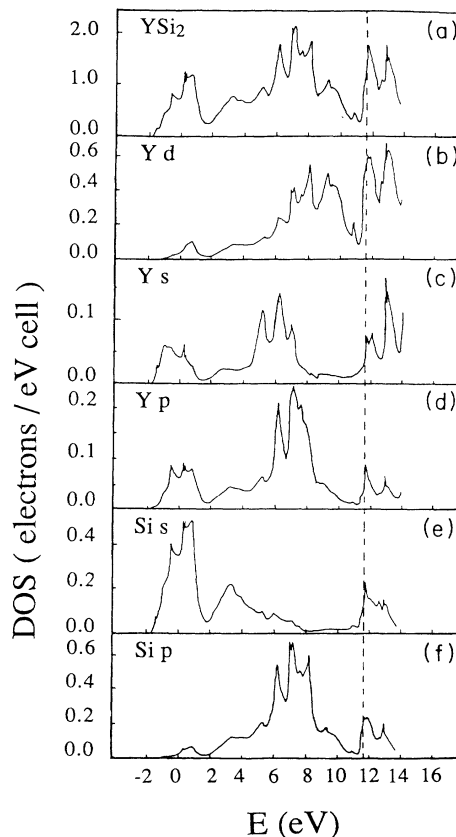


FIG. 2. APW densities of states of YSi₂. Note the variable scale for the different angular momentum components. The Si partial DOS are given for one silicon atom.

sistent with experiments³ on the related compound Gd₃Si₅. Figure 2 shows the YSi₂ total and partial densities of states. This is nearly identical to Fig. 1, which can easily be understood since YSi₂ and ErSi₂ have the same crystallographic structure and electronic configuration. These density-of-states features should be shared by the whole trivalent heavy-rare-earth disilicides family. Since the APW calculations employed the muffin-tin approximation, which could be questioned in the case of a layered structure such as the AlB₂ one, we have checked the YSi₂ results by performing full-potential linear-augmented-plane-wave (LAPW) calculations. The corresponding DOS are shown in Fig. 3. The overall agreement is good with minor differences, which are probably due to the use of a larger set of *k* points in the LAPW calculation (100 instead of 45) rather than the use of full potential instead of muffin-tin potential. Anyway, these differences are of little importance in the comparison of the theoretical results with the much broader experimental spectra.

In Figs. 1 and 2, the Fermi levels fall into a rather high density-of-states region. These values have been determined for fully stoichiometric RSi₂ ($R=\text{Er}$ or Y), with no silicon vacancies. However, there is a pseudogap very close below the Fermi level. In a rigid band-shift approximation, the effect of the silicon vacancies in the silicide

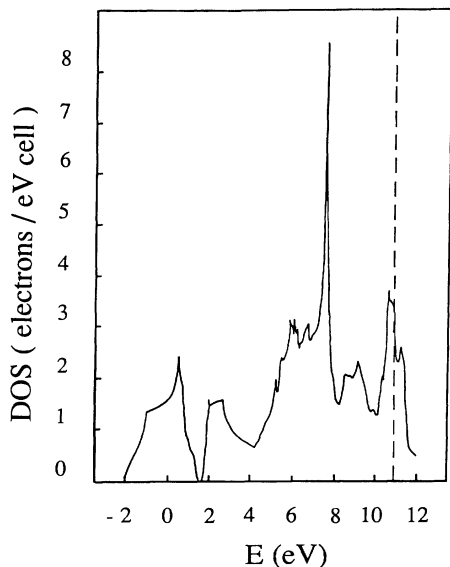


FIG. 3. Total density of states for YSi_2 computed with a full-potential APW method.

would be to shift the Fermi level toward this DOS minimum, thus stabilizing the system. We have recently confirmed this effect of the vacancies using a linear-muffin-tin orbital (LMTO) supercell calculation.

Up to now, no theoretical study of ErSi_2 electronic structure is available in the literature, but our results are in good agreement with the DOS of YSi_2 obtained by Fujitani and Asano⁹ using the LMTO-atomic-sphere approximation method.

III. EXPERIMENT

We have performed x-ray-excited Auger electron spectroscopy and x-ray photoemission spectroscopy on erbium silicide samples prepared *in situ* in a Vacuum Science Workshop apparatus (see Ref. 8 for more details about the experimental set up). We shall first describe the sample preparation procedure, and afterwards we shall present the experimental results.

A. Sample preparation

Our samples were ErSi_x layers ($x=1.7$) (Refs. 1 and 10) epitaxially grown on Si(111). The silicide films were prepared by first depositing a 30-Å-thick Er layer on a clean Si(111) substrate. A silicon capping layer was then evaporated on top of the metal film. The substrate was maintained at room temperature during Er and Si deposition. The sample was afterwards annealed at 800°C–850°C for 5–10 min to promote compound formation. We repeated this sequence of operations twice to obtain a 100-Å-thick silicide film. It has been shown that this procedure produces films with a low density of pinholes in the case of silicides epitaxially grown on Si(111) (see Ref. 15 for YSi_2 and Ref. 16 for CoSi_2). We have checked the morphology of these films by scanning electron microscopy; the surface was smooth, with a low density of pinholes (less than 5% of the surface). Our

spectra should thus be almost free of any substrate contribution (this is especially important for the Si $L_{23}VV$ spectrum). The formation of epitaxial $\text{ErSi}_{1.7}$ was attested to by the observation of the characteristic $(\sqrt{3} \times \sqrt{3})R(30)$ low-energy electron-diffraction pattern.¹⁰ The cleanliness of the sample was checked by x-ray and UV photoemission.

B. Experimental results

We first discuss the core-level line shifts between the silicide and the bulk elements (Er and Si). No noticeable shifts could be detected for the metal (Er 4*f* and Er 4*d*) core levels within our experimental accuracy (± 0.2 eV). The Si 2*p* core-level line is shifted by 0.4 eV towards lower binding energy (BE) in the silicide relative to bulk Si. The kinetic energy of the Si *KLL* Auger line is increased by 1.15 eV in the silicide relative to bulk Si. By computing the Auger parameter for Si and ErSi_x ,¹⁷ we find that the Si 2*p* BE shift is essentially due to an increased extra-atomic relaxation energy (by 0.4 eV) in the silicide, and not to an initial-state shift. From Er and Si core-level studies, we thus conclude that the charge transfer between Er and Si on the silicide should be rather weak. Our results are in agreement with previously published data on rare-earth silicides [YSi_2 ,⁵ Gd_3Si_5 ,¹⁸ and $\text{GdSi}_{1.7}$ (Ref. 19)].

Due to the presence of the 4*f* multiplet structure below 4.5 eV BE,²⁰ our valence-band XPS data are limited to the 0–4-eV BE range. The spectrum shown in Fig. 4 was acquired using a monochromatized Al *K* α line with an overall resolution of 0.5 eV (measured from the Fermi-level cutoff of an Ag sample). The Fermi-energy position was deduced from measurements of the Fermi-level cutoff and of the Ag 3*d*_{5/2} BE (368.2 eV) on a silver sample (accuracy ± 0.2 eV). It shows essentially two broad structures, centered at 0.8 and 2.5 eV and separated by shallow minima at 1.15 and 3.15 eV. No theoretical calculations exist for the photoionization cross section of the Er 5*d* in the atomic state (since the Er atom does not have

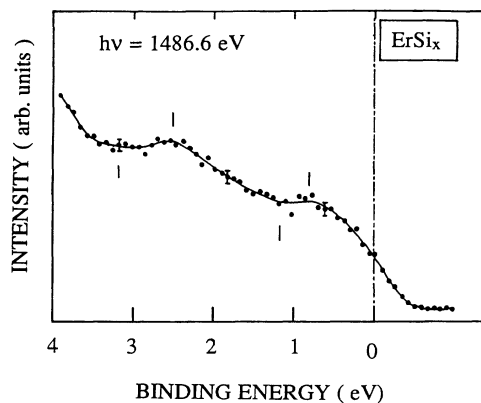


FIG. 4. X-ray photoemission spectrum of the valence band of Er silicide epitaxially grown on Si(111) (monochromatized Al-*K* α line). Dots denote experimental points. Continuous line denotes result of a cubic spline smoothing. The main structures are indicated by tic marks.

5*d* electrons), but by interpolating the existing data for Gd and Lu,²¹ we find that the “atomic” photoionization cross section of the Er 5*d* states at this photon energy should be at least five times that of the Si 3*p* states. Although the atomic cross section values must be considered with some care in the case of silicides,²² we can conclude that the Er 5*d* partial DOS should give a significant (if not dominant) contribution to our spectrum. Our spectra also resemble those published in Ref. 3 on Gd₃Si₅ at lower photon energies (except for the precise location of the Fermi level).

In order to get some information on the Si 3*p* partial DOS in the valence band, we have recorded the Si *L*₂₃*VV* Auger peak on our silicide films. A typical spectrum is shown in Fig. 5, together with the spectrum of a clean Si(111) 7×7 surface. The kinetic energy (KE) is referenced to the Fermi level and the Si 2*p* BE (which is the energy origin for the Si *L*₂₃*VV* line) is shown by arrows. One notices that the Auger peak for the silicide is more symmetric than for Si, and that it extends towards higher KE, actually up to the value corresponding to the Si 2*p* BE. Since the Si *L*₂₃*VV* line shape is very roughly given by the self-fold of the Si 3*p* partial DOS (see Sec. II B and Ref. 23) the observation of a finite (nonzero) signal just below the origin suggests that some Si 3*p*-derived states contribute to the DOS close to the Fermi level. A similar result has already been found on Tb silicide.²⁴

IV. THEORY-EXPERIMENT COMPARISON

Due to the overlap of the 4*f* multiplet components with the valence-band structures we can only compare the theoretical DOS and the experimental spectra from the Fermi level to a 4-eV BE. Because of the larger Er 5*d* photoionization cross section, the XPS spectra should be more representative of the Er 5*d* partial DOS than of the

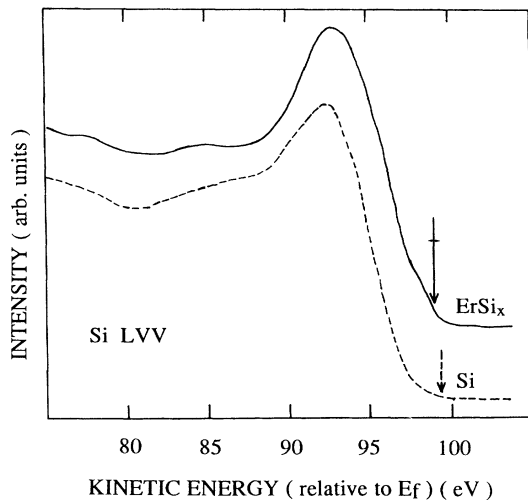


FIG. 5. Si *L*₂₃*VV* Auger spectra of a clean Si(111) 7×7 surface (dashed line) and of an epitaxial Er silicide film (continuous line). Vertical arrows indicate the binding energies of the corresponding Si 2*p* lines.

total ErSi₂ DOS. (The energy location of the main structures are identical in both the total and the partial DOS between 0 and 5-eV BE, see Fig. 1.) We can only compare the relative positions of the structure between the experimental XPS spectra of ErSi_x (Fig. 4) and the theoretical DOS of the stoichiometric ErSi₂ (Fig. 1). We identify two peaks in the Er 5*d* partial DOS (and in the total DOS) in Fig. 1, separated by 1.5–2 eV, (located around 2 and 3.5–4 eV, respectively). Those peaks may correspond to the structures observed at 0.8 and 2.5 eV in the experimental spectrum, assuming a (rigid) shift of the Fermi level by –1.2 eV for the theoretical DOS. Under this assumption, both the energy location and the character of the computed DOS structures are consistent with the findings of Ref. 3 for Gd₃Si₅ in the 0–4-eV BE range [i.e., one peak at 2.5-eV BE with mixed Si 3*p*-Gd 5*d* character and another peak close to *E*_F (≈1 eV) with a larger Gd 5*d* contribution].³

The experimental Si *L*₂₃*VV* Auger line (Fig. 5) shows a shoulder close to the origin and a peak at 6 eV rather symmetric. This is quite different from the calculated spectrum of Fig. 6, where the maximum is found around 10 eV with very little intensity close to the origin. These differences in line shape and peak positions cannot be due to correlation effects that would have the opposite effect, as found for Ca silicides.²⁵ One may invoke a matrix-element effect to explain the difference in the position of the maximum of the line between Figs. 5 and 6. This effect has been empirically accounted for in Eqs. (1) and (2) by multiplying the Si *s* partial DOS by a factor of 0.3, in order to simulate the decrease of the *ss* and *sp* contributions relative to the *pp* one that is commonly observed in silicon²³ and in silicides.²⁴ This rough way of including matrix elements may be questionable but is clear from Fig. 1 that both Si *s* and *p* partial DOS are rather small within 3 eV below the Fermi level. Thus, even if the actual weight of the *ss*, *sp*, and *pp* contributions is different from the one assumed in Eqs. (1) and (2), the maximum of the Si *L*₂₃*VV* line shape computed using the partial DOS of Fig. 1 would necessarily be located at much more than 6 eV from the origin. Matrix-element effects should thus not be responsible for the discrepancies between theory

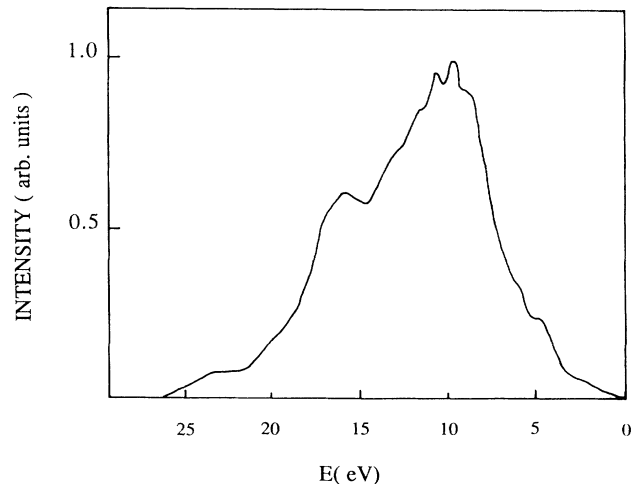


FIG. 6. Calculated Si *L*₂₃*VV* Auger spectra.

and experiment. They might be due to a surface effect, which has been observed for the Si $L_{23}VV$ line.²⁶ It is reasonable to assume that the surface structure of ErSi_x films epitaxially grown on Si(111) is the same as that of epitaxial YSi_2 layers.²⁷ The ErSi_2 layers should thus be terminated by a Si plane, with some displacement of the Si atoms. The first bulk Si plane is located at 4.1 Å from the surface, the second one at 8.2 Å, and so on. These distances are of the same order as the mean free path of the Si $L_{23}VV$ electrons (5–10 Å). Thus, the weight of the surface Si plane in the spectrum of Fig. 5 may be quite important, and if its electronic structure is very different from that of a bulk Si plane, the experimental Si $L_{23}VV$ spectrum may differ significantly from the one computed for bulk atoms. We do not really believe in this explanation, at least as far as the energy position of the main peak is concerned, for two reasons.

(i) We do not find evidence for any “bulk” structure at 10 eV from the origin in the experimental spectrum. (We find, instead, a minimum at this position.) If the above explanation were correct, it would thus imply an extremely short mean free path (certainly less than 4 Å) for Auger electrons. Moreover, surface effects are generally smaller than the one reported here for the Si $L_{23}VV$ (Ref. 26) line.

(ii) Si $L_{23}VV$ Auger spectra recorded on polycrystalline Gd_3Si_5 samples (a compound closely related to ErSi_x) agree with our results for the main peak position.²⁸ Scraped polycrystalline samples should, however, be much less sensitive to surface effects than epitaxial ones.

Therefore, surface effects should be ruled out, at least as far as the main peak position is concerned (these effects might, however, include some additional structures in the spectra). Anyway, if the Si partial DOS computed for ErSi_2 were correct for $\text{ErSi}_{1.7}$, it would be difficult to explain the large differences we observe between the experimental and simulated Si $L_{23}VV$ Auger line. In our opinion, the most plausible explanation for the above discrepancies is that the actual partial Si density of states in ErSi_x (with $x \approx 1.7$) differs significantly from that computed for stoichiometric ErSi_2 . It should be emphasized that each vacancy in the Si planes modifies the local coordination of three Si atoms, so that more than half of the existing Si atoms (three out of five) in $\text{ErSi}_{1.7}$ have only two Si atoms as nearest neighbors instead of the three in stoichiometric ErSi_2 (see Fig. 7).

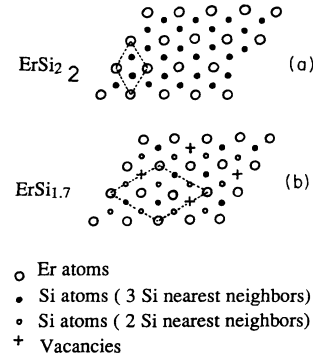


FIG. 7. Projection along the c axis of the crystallographic structure of (a) stoichiometric ErSi_2 (AlB_2 structure); (b) $\text{ErSi}_{1.7}$ (defective AlB_2). We have assumed for convenience that the vacancies are ordered in the Si planes, resulting in a $\sqrt{3} \times \sqrt{3} R(30)$ superstructure, although this has not been unambiguously proven in the case of Er silicide.¹⁰

V. CONCLUSION

We have performed APW calculations of erbium and yttrium disilicides and these results have been compared to XPS and Auger spectra. We have shown the similarity existing between ErSi_2 and YSi_2 DOS. These similarities should be shared by all members of the heavy trivalent rare-earth family. We have especially noticed an increasing Er d character near the Fermi level. A qualitative agreement is found between experimental (XPS) and theoretical valence-band results. However, differences appear in the main structure positions, both for the Auger Si LVV and the valence-band spectra.

Our experimental results are similar to those obtained for other rare-earth disilicides and our ErSi_2 APW DOS are in agreement with those of YSi_2 .⁹ The discrepancy between theory and experiment must then have an intrinsic origin. We think that the silicon vacancies play an important role, since three silicon atoms out of five are disturbed. A detailed study of their effect on the electronic structure is currently under study.

ACKNOWLEDGMENTS

This work was supported by the CNET (Centre National d'Etudes des Télécommunications) and the DRET (Direction des Recherches, Etudes et Techniques).

¹J. A. Knapp and S. T. Picraux, Appl. Phys. Lett. **48**, 466 (1986).

²K. N. Tu, R. D. Thompson, and B. Y. Tsaur, Appl. Phys. Lett. **38**, 626 (1981).

³L. Braicovich *et al.*, Phys. Rev. B **41**, 3123 (1990).

⁴P. Wetzl *et al.*, Phys. Rev. B **43**, 6620 (1991).

⁵R. Baptist, A. Pellissier, and G. Chauvet, Solid State Commun. **68**, 555 (1988).

⁶S. Valeri *et al.*, Solid State Commun. **60**, 569 (1986).

⁷G. Rossi, Surf. Sci. Rep. **7**, 1 (1987).

⁸J. Y. Veullen *et al.*, Phys. Rev. B **39**, 8015 (1989).

⁹H. Fujitani and S. Asano, *Proceedings of the International Conference on Formation of Semiconductor Interfaces 3* [Appl. Surf. Sci. **56-58**, 408 (1992)].

¹⁰F. Arnaud D'Avitaya *et al.*, Appl. Phys. Lett. **54**, 2198 (1989).

¹¹L. F. Mattheiss, J. H. Wood, and A. C. Switendick, Methods Comput. Phys. **8**, 63 (1968).

¹²L. Hedin and B. J. Lundqvist, J. Phys. C **4**, 2064 (1971).

- ¹³G. Lehmann and M. Taut, *Phys. Status Solidi B* **54**, 469 (1972).
- ¹⁴L. Calliari *et al.*, *Phys. Rev. B* **41**, 7569 (1990), and references therein.
- ¹⁵M. P. Siegal, W. R. Graham, and J. J. Santiado-Aviles, *J. Appl. Phys.* **68**, 574 (1990).
- ¹⁶A. E. M. J. Fischer, T. Gustafsson, and J. F. van der Veen, *Phys. Rev. B* **37**, 6305 (1988).
- ¹⁷See, e.g., W. F. Egelhoff, *Surf. Sci. Rep.* **6**, 253 (1987).
- ¹⁸E. Puppin, I. Lindau, and I. Abbatti, *Solid State Commun.* **77**, 983 (1991).
- ¹⁹W. A. Henle *et al.*, *Solid State Commun.* **71**, 657 (1989).
- ²⁰J. K. Lang, Y. Baer, and P. A. Cox, *J. Phys. F* **11**, 121 (1981).
- ²¹J. J. Yeh and I. Lindau, *At. Data Nucl. Data Tables* **32**, 2 (1985).
- ²²W. Speier *et al.*, *Phys. Rev. B* **39**, 6008 (1989).
- ²³D. R. Jennison, *Phys. Rev. Lett.* **40**, 807 (1978).
- ²⁴J. Y. Veuillen, S. Khennou, and T. T. A. Nguyen, *Solid State Commun.* **79**, 795 (1991).
- ²⁵O. Bisi, in *Auger Spectroscopy and Electronic Structure*, edited by G. Cubiotti, G. Mondio, and K. Wandelt, Springer Series in Surface Science Vol. 18 (Springer-Verlag, Berlin, 1989), p. 30.
- ²⁶S. M. Durbin and T. Gog, *Phys. Rev. Lett.* **63**, 1304 (1989).
- ²⁷R. Baptist *et al.*, *Phys. Rev. Lett.* **64**, 311 (1990).
- ²⁸M. Sancrotti *et al.*, in *Auger Spectroscopy and Electronic Structure* (Ref. 25), p. 116.